PERGAMON

International Journal of Heat and Mass Transfer 46 (2003) 761–769

International Journal of HEAT and MASS TRANSFER

www.elsevier.com/locate/ijhmt

Heat transfer analysis of mutually irradiating fins

C.K. Krishnaprakas, K. Badari Narayana *

Thermal Systems Group, ISRO Satellite Centre, Vimanapura Post, Bangalore 560 017, India

Received 22 March 2002; received in revised form 28 August 2002

Abstract

Apparent emittance of a longitudinal rectangular fin system with an opening angle, accounting fin-to-fin radiation interaction and also with surfaces that reflect radiation in both diffuse and specular regimes has been evaluated. The governing equation of the problem is a complicated integro-differential equation. This equation has been solved with the Gauss–Jacobi orthogonal collocation method, which possesses the quality of exceptional accuracy with a few numbers of nodes. Finally, the minimum mass design of the fin has been arrived at.

1. Introduction

Radiating fins are used in spacecraft and space vehicles to reject waste heat generated from the various components to the cold space. Since weight reduction is important for space vehicles, it is necessary to obtain accurately the heat transfer rates of the radiators to achieve at optimum design. Gallinan and Berggren [1] discuss various design criteria associated with radiators for space vehicle. Analysis of radiating fins has been the subject of research by a number of investigators. However, much of the work in this area is limited to single fins freely radiating to space. Only a few investigators have considered the optimum design of a radiating fin array considering mutual interactions between the radiating elements. Sparrow et al. [2] and Sparrow and Eckert [3] presented the optimum design of radiatively interacting longitudinal fins considering fin-to-fin interaction but for fully diffuse reflecting surfaces [1,2]. The work by Karlekar and Chao [4] focussed on diffuse surfaces while analyzing the optimum design of trapezoidal fins. Hering [5] and Tien [6] considered the mutual radiation interaction between conducting plates for fully specular surfaces. Schnurr et al. [7] also considered only diffusely reflecting surfaces. Love and Francis [8] presented an analysis using linearized radiative heat transfer coefficient for the case of fully specularly reflecting fins. They provided an approximate solution for radiative-convective fins. Chung and Zhang [9,10] using a variational calculus approach determined the optimum shape and minimum mass of a thin fin with diffuse reflecting surfaces. Krishnaprakas [11] presented the optimum design of a diffusely reflecting rectangular plate fin array extending from a plane wall employing a nonlinear optimization method. Thermodynamic optimization of tubular space radiators is discussed by Balaji et al. [12], however without considering the effect of specular interreflections.

Mass minimization studies of radiative fin arrays are dealt by only few investigators. Similarly studies of radiation considering specular and/or diffuse effects also are rather scarce. To our knowledge this is the first paper to consider them together. It is the purpose of the present analysis to determine the temperature profile and heat flux in a longitudinal rectangular fin system with an opening angle accounting fin-to-fin radiation interaction and also with surfaces that reflect radiation in both diffuse and specular regimes. The resulting governing equation, that is a complicated integro-differential equation, has been solved with the Gauss–Jacobi orthogonal collocation method (GJOCM), which possesses the quality of exceptional accuracy with a few number of nodes. This is the first time in radiation literature that the GJOCM is used. Finally, the minimum mass design of the fin has been arrived at.

* Corresponding author. Tel.: +91-008-5083-104; fax: +91-008-508-3203.

E-mail address: kbn@isac.ernet.in (K. Badari Narayana).

0017-9310/03/$ - see front matter © 2002 Elsevier Science Ltd. All rights reserved.
PII: S0017-9310(02)00356-3

Nomenclature

A_p	profile area of the fin (m^2)
C	GJOCM second derivative weight matrix
D	GJOCM first derivative weight matrix
$dF_{dx1-dx2}$	elemental view factor from dx_1 to dx_2
$dF_{d\xi-d\xi'}$	elemental view factor from $d\xi$ to $d\xi'$
J	radiosity (W/m^2)
J	Jacobian matrix
k	thermal conductivity of fin material (W/m K)
K	kernel matrix, see Eq. (22)
L	fin length (m)
N_c	conduction–radiation number $= kt/\sigma T_b^3 L^2$
q	rate of total heat transfer from the fin (W/m^2)
q'	rate of total heat transfer from the fin (W/m^2)
t	semi-thickness of the fin (m)
T	temperature of the fin (K)
T_b	temperature at the fin base (K)
$\boldsymbol{w}^{GL}$	Gauss–Lobatto weight vector
$\boldsymbol{w}^{R}$	Radau weight vector
W	Integration weight matrix, see Eq. (23)
x	coordinate along the length of the fin measured from the base (m)

Greek symbols

β	dimensionless radiosity $= J/\sigma T_b^4$
γ	fin opening angle, degree
ε	emittance of fin surface
ε_{app}	apparent emittance
ρ	surface reflectance $= 1-\varepsilon$
ρ^s	specular reflectance $= \varsigma\rho$
ρ^d	diffuse reflectance $= (1-\varsigma)\rho$
σ	Stefan–Boltzmann constant (5.67×10^{-8} W/m^2 K^4)
θ	dimensionless temperature $= T/T_b$
ς	specularity rate $= \rho^s/\rho$
ξ	dimensionless coordinate $= x/L$

Subscripts

1,2	fin number description
b	fin base
opt	optimum

Abbreviation

GJOCM	Gauss–Jacobi orthogonal collocation method

2. Mathematical model

Fig. 1 shows a schematic diagram of the configuration of fin array considered in the present analysis, i.e., a number of longitudinal fins extending from a cylindrical base with an opening angle between two. The coordinate system used is depicted in Fig. 2. The base area is so small that its radiation interaction with the fin is ignored. The following assumptions are made: (1) one dimensional steady state heat flow (thin fin assumption) for profile of uniform thickness is considered, (2) gray, diffusely emitting radiating surfaces, (3) the reflectance of the surface is composed of a simple sum of the diffuse and specular components, i.e., $\rho = 1-\varepsilon = \rho^d + \rho^s$, (4) no incident loads from any external sources, (5) surroundings at absolute zero temperature, (6) the temperature and radiosity distribution with respect to length are the same in every fin, i.e., symmetry condition, and (7) constant thermal conductivity and emittance.

Under steady state conditions the energy conservation law requires that the net heat flux conducted across the differential element δx should be equal to the net radiative flux absorbed by δx from the adjacent fin and from the same fin in view of self-radiation view factor [13,14]. The governing differential equation for the temperature distribution of the fin may be written along with the boundary conditions as:

$$\frac{d^2T_1}{dx_1^2} = \frac{1}{kt}\left[J_1(x_1) - (1-\rho^s)\int_{x_2=0}^{L} J_2(x_2)\,dF^s_{dx_1-dx_2} - (1-\rho^s)\int_{x_1'=0}^{L} J_1(x_1')\,dF^s_{dx_1-dx_1'}\right] \quad (1)$$

$$T_1(x_1=0) = T_b, \quad -k2t\left.\frac{dT_1(x_1)}{dx_1}\right|_{x_1=L} = 2t\varepsilon\sigma T^4(x_1=L) \quad (2)$$

where the radiosity along fin-1 follows the relation

$$J_1(x_1) = \varepsilon\sigma T_1^4(x_1) + \rho^d\int_{x_2=0}^{L} J_2(x_2)\,dF^s_{dx_1-dx_2} + \rho^d\int_{x_1'=0}^{L} J_1(x_1')\,dF^s_{dx_1-dx_1'} \quad (3)$$

The specular radiation view factors are evaluated as

$$dF^s_{dx_1-dx_2} = dF_{dx_1-dx_2,\gamma} + (\rho^s)^2\,dF_{dx_1(1,2)-dx_2,3\gamma} + (\rho^s)^4\,dF_{dx_1(1,2,1,2)-dx_2,5\gamma} + \cdots \quad (4)$$

$$dF^s_{dx_1-dx_1'} = \rho^s dF_{dx_1(2)-dx_1',2\gamma} + (\rho^s)^3 dF_{dx_1(2,1,2)-dx_1',4\gamma} + (\rho^s)^5 dF_{dx_1(2,1,2,1,2)-dx_1',6\gamma} + \cdots \quad (5)$$

The direct diffuse view factor between two fins with an opening angle γ is given by the expression [13]

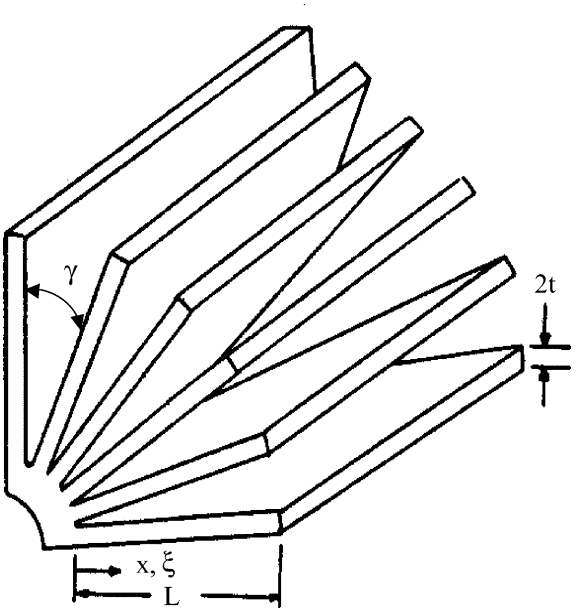

Fig. 1. Schematic diagram of fin system.

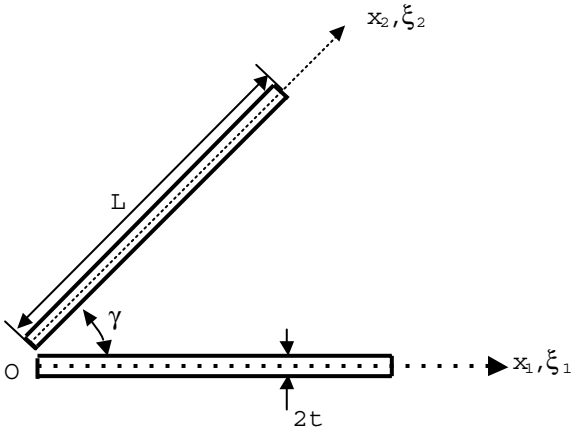

Fig. 2. Coordinate system.

$$dF_{dx_1-dx_2,\gamma} = \frac{1}{2}\frac{x_1 x_2 \sin^2\gamma}{(x_1^2 - 2x_1x_2\cos\gamma + x_2^2)^{3/2}}\,dx_2 \tag{6}$$

The total hemispherical reflectance of the fin surface is composed as a simple sum of the diffuse and specular reflectance as

$$\rho = \rho^d + \rho^s = 1 - \varepsilon \tag{7}$$

A term specularity rate is defined as the ratio of the specular reflectance to the hemispherical reflectance as

$$\varsigma = \frac{\rho^s}{\rho} \tag{8}$$

The radiative heat flux per unit area from one surface of a fin is written as

$$q'(x_1) = J_1(x_1) - (1-\rho^s)\int_{x_2=0}^{L} J_2(x_2)\,dF^s_{dx_1-dx_2} - (1-\rho^s)\int_{x_1'=0}^{L} J_1(x_1')\,dF^s_{dx_1-dx_1'} \tag{9}$$

The total radiative heat loss per unit width from both the sides of a fin is

$$q = 2\int_{x_1=0}^{L} q'^r(x_1)\,dx_1 \tag{10}$$

Alternatively, the total heat loss may be written as

$$q = -k2t\left.\frac{dT_1(x_1)}{dx_1}\right|_{x_1=0} \tag{11}$$

The effectiveness of the fin is expressed through a term called *apparent emittance* defined as the ratio of the actual total radiative heat loss to the ideal heat loss by a black, isothermal fin.

$$\varepsilon_{app} = \frac{q}{q_{ideal}} \tag{12}$$

$$q_{ideal} = 2L\sin\left(\frac{\gamma}{2}\right)\sigma T_b^4 \tag{13}$$

Substitution of Eq. (3) in Eq. (1) results in

$$\frac{d^2T_1}{dx_1^2} = \frac{1}{kt}\left[\varepsilon\sigma T_1^4(x_1) + (\rho^d+\rho^s-1)\int_{x_2=0}^{L} J_2(x_2)\,dF^s_{dx_1-dx_2} + (\rho^d+\rho^s-1)\int_{x_1'=0}^{L} J_1(x_1')\,dF^s_{dx_1-dx_1'}\right] \tag{14}$$

The governing differential equation for the temperature distribution of the fin may be written in terms of dimensionless variables as:

$$\frac{d^2\theta_1}{d\xi_1^2} = \frac{\varepsilon}{N_c}\left[\theta_1^4(\xi_1) - \int_{\xi_2=0}^{1}\beta_2(\xi_2)\,dF^s_{d\xi_1-d\xi_2} - \int_{\xi_1'=0}^{1}\beta_1(\xi_1')\,dF^s_{d\xi_1-d\xi_1'}\right] \tag{15}$$

where the dimensionless variables are defined as $\theta_1 = T_1/T_b$, $\xi_1 = x_1/L$, $\xi_2 = x_2/L$, $\beta_1 = J_1/\sigma T_b^4$, $\beta_2 = J_2/\sigma T_b^4$ and $N_c = kt/L^2\sigma T_b^3$.

Invoking symmetry conditions $\theta_1 = \theta_2$ and $\beta_1 = \beta_2$ and dropping the subscripts for the sake of brevity, Eq. (15) takes finally the form

$$\frac{d^2\theta}{d\xi^2} = \frac{\varepsilon}{N_c}\left[\theta^4(\xi) - \int_{\xi'=0}^{1} K_\gamma(\xi,\xi')\beta(\xi')\,d\xi'\right] \tag{16}$$

Radiosity variation (Eq. (3)) also is expressed in dimensionless form as

$$\beta = \varepsilon\theta^4 + \rho^{\mathrm{d}} \int_0^1 K_\gamma(\xi,\xi')\beta\,\mathrm{d}\xi \tag{17}$$

The boundary conditions, Eq. (2), in dimensionless form become

$$\theta(\xi=0)=1, \quad -\left.\frac{\mathrm{d}\theta(\xi)}{\mathrm{d}\xi}\right|_{\xi=1} = \frac{\varepsilon}{N_{\mathrm{c}}}\frac{t}{L}\theta^4(\xi=1) \tag{18}$$

The kernel K_γ of the integral function required in Eqs. (16) and (17) is defined as

$$K_\gamma(\xi,\xi') = \sum_{r=1}^{m} (\rho^{\mathrm{s}})^{(r-1)} \frac{1}{2} \frac{\xi\xi' \sin^2 r\gamma}{\left(\xi^2 - 2\xi\xi'\cos r\gamma + \xi'^2\right)^{3/2}},$$
$$\frac{180}{m+1} \leqslant \gamma < \frac{180}{m} \tag{19}$$

The variable m determines the total number of specular reflections possible. Eq. (19) is a representation of the fact that, no more radiation interaction through specular interreflections is possible when the opening angle between the fin and the specular image of itself or the adjacent fin becomes more than 180°.

The apparent emittance (see Eq. (12)) now takes the form

$$\varepsilon_{\mathrm{app}} = \frac{-N_{\mathrm{c}}}{\sin(\gamma/2)} \left.\frac{\mathrm{d}\theta}{\mathrm{d}\xi}\right|_{\xi=0} \tag{20}$$

We see from Eq. (20) that $\varepsilon_{\mathrm{app}}$ is a function of four variables, i.e., $\varepsilon_{\mathrm{app}} = \varepsilon_{\mathrm{app}}(\gamma, \varepsilon, \varsigma, N_{\mathrm{c}})$.

3. Numerical scheme

The mathematical model for the conduction–radiation interaction problem in fins has taken the form of a coupled nonlinear integro-differential system, Eqs. (16) and (17) together with the boundary conditions, Eq. (18). Sparrow et al. [2] solved these equations, for the pure diffuse case, $\rho^{\mathrm{s}} = 0$, using a finite difference scheme in which the integral part is solved using the Nystrom method employing the Simpson's compound rule of quadrature. Hering [5] solved the equations for the pure specular case, $\rho^{\mathrm{d}} = 0$, by converting the integro-differential equations, Eq. (16) into a single integral equation, and then applying an iterative method. Tien [6] also solved approximately the pure specular case using the Karman–Pohlhausen technique generally employed for the solution of boundary layer flow problems.

In the present case, the coupled nonlinear integro-differential equation, Eq. (16), is solved using the method of Gauss–Jacobi orthogonal collocation method (GJOCM) to obtain the temperature distribution in the fin. GJOCM is a finite difference scheme used to solve boundary value problems in ordinary differential equations (BVP-ODEs) in which the nodal points are taken to be the roots of the Jacobi polynomials that have the property of orthogonality in the range {0–1}. GJOCM has been extensively used in solving integro-differential equations encountered in chemical engineering problems [15,16]. An important advantage of the method is that, an exceptionally accurate solution is obtained with fewer numbers of nodes. In GJOCM, the definite integral term in the equation is substituted with a suitable Gauss–Jacobi quadrature rule including one or both of the end points, depending upon the type of weight function appearing under the integral term. This is nothing but the application of the Nystrom method widely used to solve integral equations. The derivative terms in the equation are also replaced with appropriate weight matrices [15,16]. GJOCM is now applied to Eq. (17) to obtain

$$\boldsymbol{\beta} = \varepsilon\boldsymbol{\theta}^4 + \rho^{\mathrm{d}}\mathbf{K}\mathbf{W}\boldsymbol{\beta} \tag{21}$$

where $\boldsymbol{\beta}$ and $\boldsymbol{\theta}$ are the n-dimensional column vectors containing respectively the nodal radiosity and temperature values at the n nodal points $\xi = \{\xi_1, \xi_2, \xi_3, \ldots, \xi_n\}^t$,

$$\boldsymbol{\beta} = \{\beta_i, i=1,n\}^t, \quad \boldsymbol{\theta} = \{\theta_i, i=1,n\}^t,$$
$$\boldsymbol{\theta}^4 = \{\theta_i^4, i=1,n\}^t,$$

$$\mathbf{K} = \left[k_{i,j} = \sum_{r=1}^{m} (\rho^{\mathrm{s}})^{(r-1)} \frac{1}{2} \frac{\xi_i\xi_j \sin^2 r\gamma}{(\xi_i^2 - 2\xi_i\xi_j\cos r\gamma + \xi_j^2)^{3/2}}, \quad i=1,n, \;\; j=1,n \right] \tag{22}$$

$$\mathbf{W} = \begin{bmatrix} w_{1,j} = w_j^{\mathrm{R}}, & j=1,n \\ w_{i,j} = w_j^{\mathrm{GL}}, & i=2,n, \;\; j=1,n \end{bmatrix} \tag{23}$$

The n nodal points $\xi = \{\xi_1, \xi_2, \xi_3, \ldots, \xi_n\}^t$ and the weights $\boldsymbol{w}^{\mathrm{GL}} = \{w_1^{\mathrm{GL}}, w_2^{\mathrm{GL}}, w_3^{\mathrm{GL}}, \ldots, w_n^{\mathrm{GL}}\}^t$ are taken to be the Gauss–Lobatto quadrature abscissae and weights. Gauss–Lobatto quadrature is a special case of the Gauss–Jacobi quadrature in which both the end points of the integration range are included. An arbitrary function $f(\xi)$ is numerically integrated within the limits {0–1} using the Gauss–Lobatto scheme as [17]

$$\int_0^1 f(\xi)\,\mathrm{d}\xi = w_1^{\mathrm{GL}} f(0) + \sum_{i=2}^{n-1} w_i^{\mathrm{GL}} f(\xi_i^{\mathrm{GL}}) + w_n^{\mathrm{GL}} f(1) - \frac{n(n-1)^3 2^{2n-1} n[(n-2)!]^4}{(2n-1)[(2n-1)!]^3} f^{(2n-2)}(\zeta), \quad 0<\zeta<1 \tag{24}$$

The error term in Eq. (24) demonstrates that, polynomials as high degree as $(2n-3)$ are exactly integrated with just n sampling points highlighting the superior accuracy of the method in comparison with any other quadrature schemes including the end points. Gauss–Lobatto sampling points are the roots of the first de-

rivative of the Legendre polynomial of order $(n-1)$, i.e., $P'_{n-1}(\xi)$. The first row of the weight matrix $\mathbf{W}$ is taken to be that of a Radau integration scheme, but employing the same Gauss–Lobatto abscissas skipping the point $\xi = 0$ in order to circumvent the singularity of the kernel K_γ at the origin. In the Radau scheme the integration is carried out as

$$\int_0^1 f(\xi)\,\mathrm{d}\xi \approx \sum_{i=2}^{n-1} w_i^{\mathrm{R}} f(\xi_i^{\mathrm{GL}}) + w_n^{\mathrm{R}} f(1), \quad w_1^{\mathrm{R}} = 0 \tag{25}$$

The Radau integration weights w_i^{R} are evaluated by integrating individually the Lagrange interpolant functions passing through the nodal points $\xi_2, \xi_3, \ldots, \xi_n$ (note that the point $\xi_1 = 0$ is omitted). Eq. (21) implies that

$$\boldsymbol{\beta} = \varepsilon[\mathbf{I} - \rho^{\mathrm{d}}\mathbf{KW}]^{-1}\boldsymbol{\theta}^4 \tag{26}$$

Applying GJOCM to Eq. (16) and using the relation, Eq. (24), results in

$$\begin{aligned}\mathbf{C}\boldsymbol{\theta} &= \frac{\varepsilon}{N_{\mathrm{c}}}[\boldsymbol{\theta}^4 - \mathbf{KW}\boldsymbol{\beta}] \\ &= \frac{\varepsilon}{N_{\mathrm{c}}}[\boldsymbol{\theta}^4 - \varepsilon\mathbf{KW}[\mathbf{I} - \rho^{\mathrm{d}}\mathbf{KW}]^{-1}\boldsymbol{\theta}^4]\end{aligned} \tag{27}$$

where $\mathbf{C}$ is the second derivative weight matrix $\mathbf{C} = [c_{i,j}]$ such that

$$\boldsymbol{\theta}'' = \left\{ \left.\frac{\mathrm{d}^2\theta}{\mathrm{d}\xi^2}\right|_{\xi=\xi_1}, \left.\frac{\mathrm{d}^2\theta}{\mathrm{d}\xi^2}\right|_{\xi=\xi_2}, \left.\frac{\mathrm{d}^2\theta}{\mathrm{d}\xi^2}\right|_{\xi=\xi_3}, \ldots, \left.\frac{\mathrm{d}^2\theta}{\mathrm{d}\xi^2}\right|_{\xi=\xi_n} \right\}^t = \mathbf{C}\boldsymbol{\theta} \tag{28}$$

$\mathbf{D}$, the first derivative weight matrix that is needed while handling the boundary condition at $\xi = 1$ (Eq. (18)), is defined as

$$\boldsymbol{\theta}' = \left\{ \left.\frac{\mathrm{d}\theta}{\mathrm{d}\xi}\right|_{\xi=\xi_1}, \left.\frac{\mathrm{d}\theta}{\mathrm{d}\xi}\right|_{\xi=\xi_2}, \left.\frac{\mathrm{d}\theta}{\mathrm{d}\xi}\right|_{\xi=\xi_3}, \ldots, \left.\frac{\mathrm{d}\theta}{\mathrm{d}\xi}\right|_{\xi=\xi_n} \right\}^t = \mathbf{D}\boldsymbol{\theta} \tag{29}$$

Eq. (27) is rearranged as

$$\mathbf{C}\boldsymbol{\theta} - \frac{\varepsilon}{N_{\mathrm{c}}}[\mathbf{I} - \varepsilon\mathbf{KW}[\mathbf{I} - \rho^{\mathrm{d}}\mathbf{KW}]^{-1}]\boldsymbol{\theta}^4 = \mathbf{f}(\boldsymbol{\theta}) = 0 \tag{30}$$

Evaluation of the derivative weight matrices is explained by Villadsen and Michelsen [16] and the weights are tabulated in the treatise by Finlayson [15]. Application of GJOCM discretization of the integro-differential system Eqs. (16) and (17) has finally led to a set of nonlinear algebraic equations, Eq. (30). Newton-Raphson method is employed to solve these equations iteratively to obtain the $(k+1)$th iterate form the kth iterate as [17]

$$\boldsymbol{\theta}^{(k+1)} = \boldsymbol{\theta}^{(k)} - \mathbf{J}^{-1}(\boldsymbol{\theta}^{(k)})\mathbf{f}(\boldsymbol{\theta}^{(k)}) \tag{31}$$

$\mathbf{J}(\boldsymbol{\theta})$ is the Jacobian matrix of the nonlinear system $\mathbf{f}(\boldsymbol{\theta})$, and is evaluated as

$$\mathbf{J}(\boldsymbol{\theta}^{(k)}) = \mathbf{C} - \frac{4\varepsilon}{N_{\mathrm{c}}}[\mathbf{I} - \varepsilon\ \mathbf{KW}[\mathbf{I} - \rho^{\mathrm{d}}\mathbf{KW}]^{-1}]\boldsymbol{\theta}^{(k)^3} \tag{32}$$

The Newton–Raphson iterative process is repeated until convergence, i.e., when the maximum norm of the relative difference between two successive iterates is within a tolerance of 10^{-5}.

Finally the apparent emittance is obtained from the nodal temperatures as

$$\varepsilon_{\mathrm{app}} = \frac{-N_{\mathrm{c}}}{\sin(\gamma/2)} \left.\frac{\mathrm{d}\theta}{\mathrm{d}\xi}\right|_{\xi=0} = \frac{-N_{\mathrm{c}}}{\sin(\gamma/2)} \sum_{j=1}^{n} d_{1,j}\theta_j \tag{33}$$

4. Optimum design

The optimum design of a fin array accomplishes the maximum overall heat transfer from the fin to the surroundings for a given fin mass or profile area A_{p}. We assume that all other parameters ε, k and T_{b} are known. Therefore, a particular combination of L and t_{b} out of all possible combinations gives the maximum heat transfer keeping A_{p} a constant. This means that, in terms of dimensionless quantities, $\varepsilon_{\mathrm{app}} = \varepsilon_{\mathrm{app}}(\gamma, \varepsilon, \varsigma, N_{\mathrm{c}})$ should be maximum for a an optimum value of N_{c}, denoted as N_{c}^* under specified values of γ, ε, ς, k, T_{b} and A_{p}.

The fin profile area is

$$A_{\mathrm{p}} = 2tL \tag{34}$$

The heat loss from the fin is written after some algebraic manipulations, as

$$\begin{aligned} q &= \varepsilon_{\mathrm{app}} q_{\mathrm{ideal}} = \varepsilon_{\mathrm{app}} 2L \sin\left(\frac{\gamma}{2}\right)\sigma T_{\mathrm{b}}^4 \\ &= 4^{1/3} A_{\mathrm{p}}^{1/3} \sigma^{2/3} T_{\mathrm{b}}^3 k^{1/3} \frac{\varepsilon_{\mathrm{app}}}{N_{\mathrm{c}}^{1/3}} = \mathrm{const}\,\frac{\varepsilon_{\mathrm{app}}}{N_{\mathrm{c}}^{1/3}} \end{aligned} \tag{35}$$

The constrained optimization problem may now be stated mathematically as

$$\begin{aligned} &\text{For given} \quad \gamma, \varepsilon, \varsigma, k, T_{\mathrm{b}} \text{ and } A_{\mathrm{p}} \\ &\text{maximize} \quad f(N_{\mathrm{c}}) = \frac{\varepsilon_{\mathrm{opt}}(\gamma, \varepsilon, \varsigma, N_{\mathrm{c}})}{N_{\mathrm{c}}^{1/3}} \end{aligned} \tag{36}$$

The one-dimensional optimization problem, Eq. (36) is solved using the Powell's quadratic search algorithm [18].

5. Results and discussion

The results of the analysis are plotted against that reported by Sparrow et al. [2] for the case of pure diffuse

reflection and that reported by Hering [5] for the case of pure specular reflection, in Fig. 3. Good agreement between the results has been observed confirming the validity of the present numerical modelling. Fig. 4 displays the effect of opening angle on the performance of fin for the fully specular case. At smaller opening angles fin performs better. As the specularity rate increases, the fin performance improves, as demonstrated in Fig. 5. The effect of specular reflection is more predominant at smaller opening angles and at intermediate values of emittances as observed in Fig. 6. Fig. 7 depicts the variation of apparent emittance at different specularity levels. Specularity rate has an effect of almost linear variation on the fin performance as revealed in Fig. 8, at all emittance values. The results of grid independence studies are presented in Figs. 9 and 10. It appears that, at smaller opening angles refined grid is needed. Also, diffuse surface models need more nodal points than specular surface models. 40 numbers of grids is sufficient to obtain accurate results in most cases. Even 5 numbers of nodes fetches accurate results for an opening angle 40°. Figs. 9 and 10 also display the smooth trend in which the solution converges as the numerical grid becomes finer. No convergence difficulties were experienced with the present numerical scheme. Optimum N_c values, at which the apparent emittance becomes maximum for a given profile area, are presented in Fig. 11.

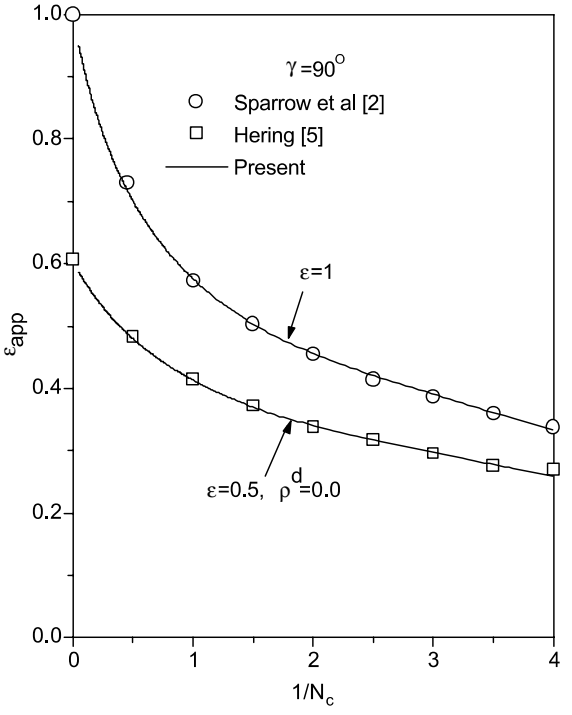

Fig. 3. Comparison of solutions.

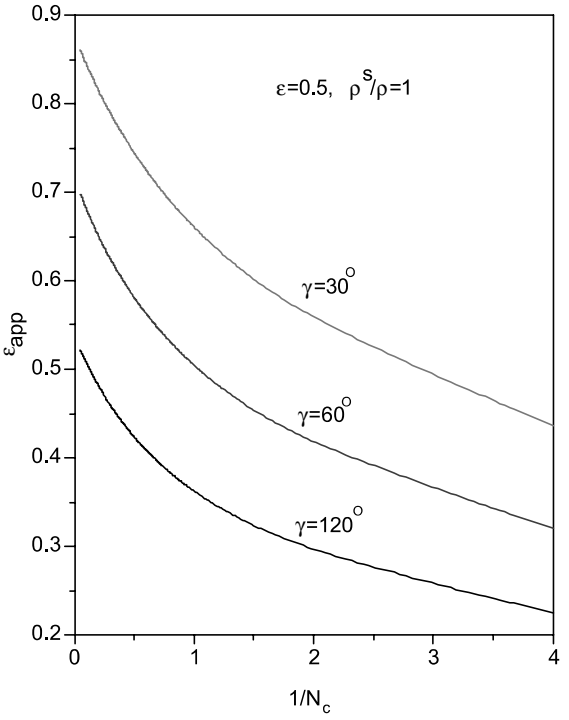

Fig. 4. Effect of parameter N_c.

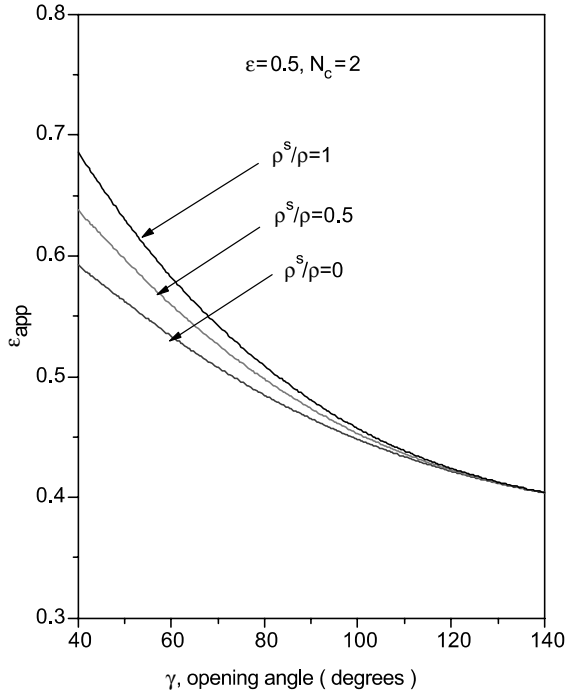

Fig. 5. Effect of angle between fins.

Optimum N_c does not seem to be affected significantly by whether the surface is diffuse or specular. However,

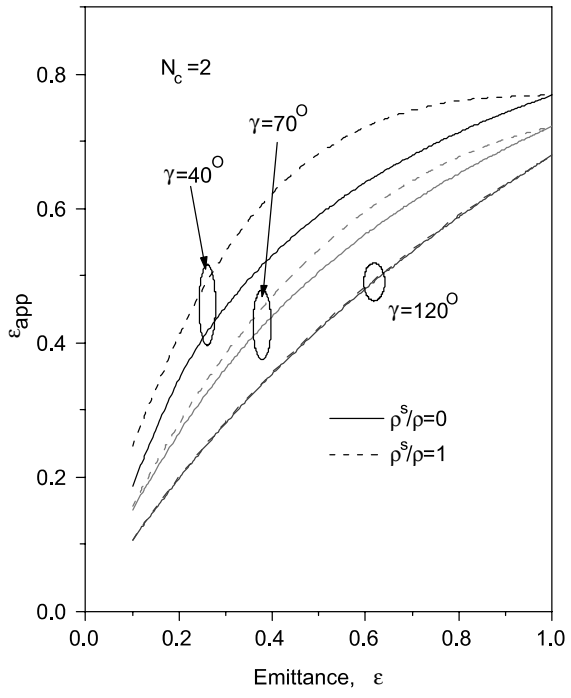

Fig. 6. Effect of emittance.

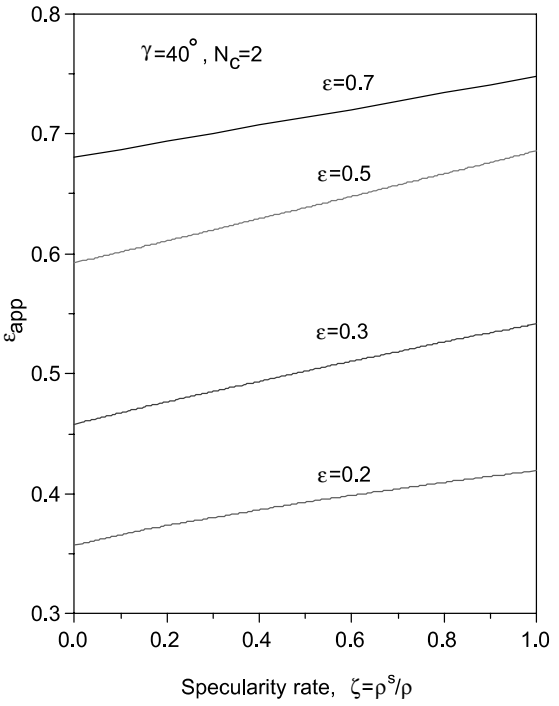

Fig. 8. Effect of specularity rate.

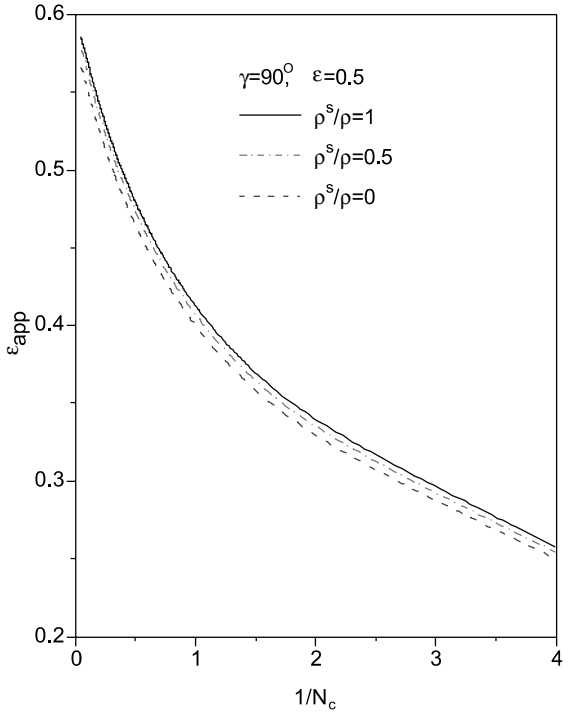

Fig. 7. Effect of specular reflection.

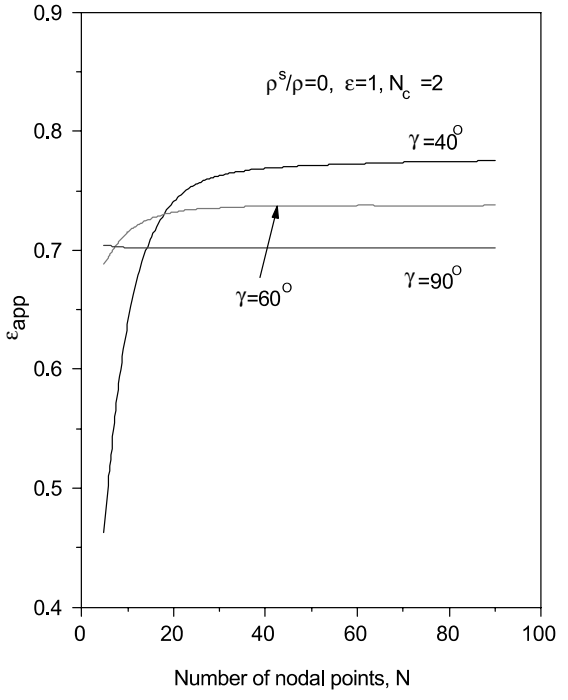

Fig. 9. Effect of grid size (diffuse case).

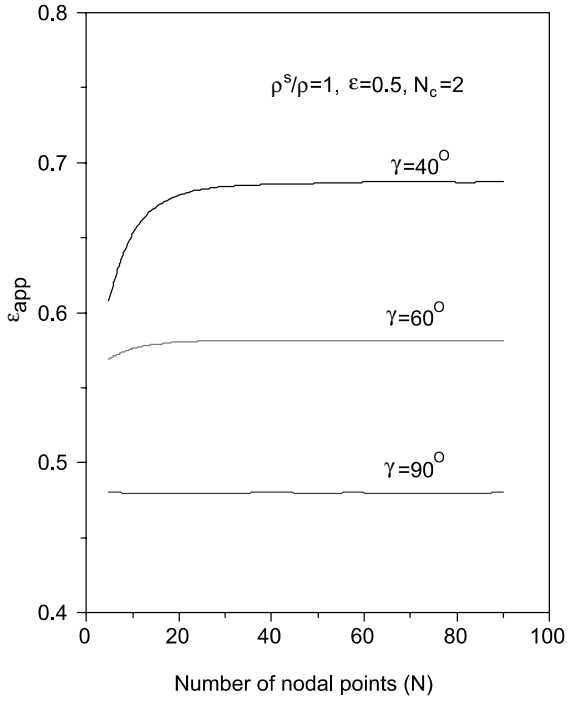

Fig. 10. Effect of grid size (specular case).

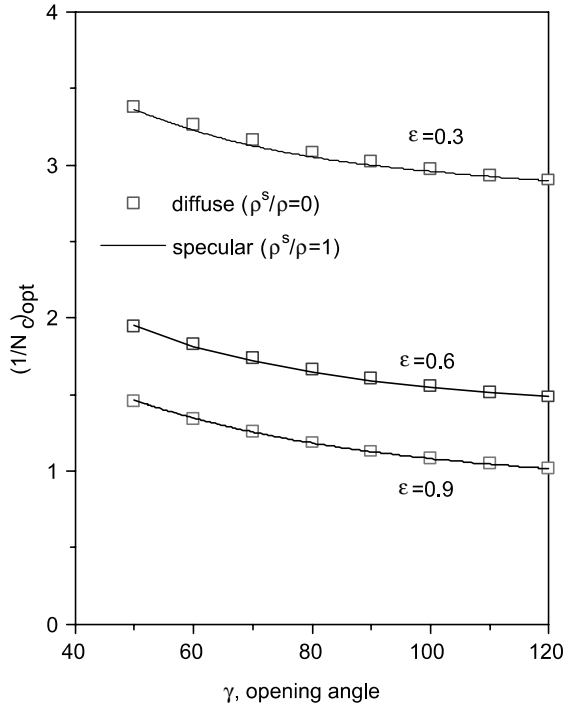

Fig. 11. Optimum N_c.

optimum N_c for specular case is slightly more than diffuse case. This implies that radiation interaction is little less for the specular reflection case than the diffuse reflection case at the optimum profile of the fin.

6. Conclusions

Apparent emittance of a longitudinal rectangular fin system accounting fin-to-fin radiation interaction and also with surfaces that reflect radiation in both diffuse and specular regimes, has been evaluated. The governing equation, that is a complicated integro-differential equation, has been solved using GJOCM, which possesses exceptional accuracy using fewer numbers of nodes. The optimum dimensions of the fin have been arrived at. GJOCM can also be efficiently used for fin systems having different profiles like triangular, parabolic etc.

Acknowledgements

The authors wish to thank D.R. Bhandari, Head, Thermal Design and Analysis Division, H. Narayanamurthy, Group Director, Thermal Systems Group and Prof. A.V. Patki, Deputy Director, ISRO Satellite Centre, for their support and encouragement during the course of this work.

References

[1] J.P. Gallinan, W.P. Berggren, Some radiator design criteria for space vehicles, ASME J. Heat Transfer 81C (1959) 237–238.
[2] E.M. Sparrow, E.R.G. Eckert, T.F. Irvine Jr., The effectiveness of radiating fins with mutual irradiation, J. Aerospace Sci. 28 (1961) 763–772.
[3] E.M. Sparrow, E.R.G. Eckert, Radiant interaction between fin and base surfaces, J. Heat Transfer 84 (1962) 12–18.
[4] B.V. Karlekar, B.T. Chao, Mass minimization of radiating trapezoidal fins with negligible base cylinder interaction, Int. J. Heat Mass Transfer 6 (1963) 33–48.
[5] R.G. Hering, Radiative heat exchange between conducing plates with specular reflection, ASME J. Heat Transfer 88C (1966) 29–36.
[6] C.L. Tien, Approximate solutions of radiative exchange between conducting plates with specular reflection, ASME J. Heat Transfer 89C (1967) 119–120.
[7] N.M. Schnurr, A.B. Shapiro, M.A. Townsend, Optimization of radiating fin arrays with respect to weight, ASME J. Heat Transfer 98 (1976) 643–648.
[8] T.J. Love, J.E. Francis, in: R. Viskanta (Ed.), A linearized analysis for longitudinal fins with radiative and convective exchange, Thermophysics and thermal control Progress in Astronautics and Aeronautics, vol. 65, AIAA, 1979, pp. 242–252.

[9] B.T.F. Chung, B.X. Zhang, Minimum mass longitudinal fins with radiation interaction at the base, J. Franklin Inst. 328 (1) (1991) 143–161.
[10] B.T.F. Chung, B.X. Zhang, Optimization of radiating fin array including mutual irradiations between radiator elements, ASME J. Heat Transfer 113 (1991) 814–822.
[11] C.K. Krishnaprakas, Optimum design of radiating rectangular plate fin array extending from a plane wall, ASME J. Heat Transfer 118 (1996) 490–493.
[12] C. Balaji, K. Sri Jayaram, S.P. Ventateshan, Thermodynamic optimization of tubular space radiators, AIAA J. Thermophys. Heat Transfer 10 (9) (1996) 705–707.
[13] M.N. Ozisik, Radiative Transfer and Interactions with Conduction and Convection, Wiley, New York, 1973.
[14] M.F. Modest, Radiative Heat Transfer, McGraw-Hill, New York, 1993.
[15] B.A. Finlayson, The Method of Weighted Residuals and Variational Principles, Academic Press, New York, 1972.
[16] J. Villadsen, M.L. Michelsen, Solution of Differential Equation Models by Polynomial Approximation, Prentice Hall, Englewood Cliffs, NJ, 1978.
[17] A. Ralston, A First Course in Numerical Analysis, McGraw-Hill Book Company, New York, 1965.
[18] P.E. Gill, W. Murray, M.H. Wright, Practical Optimization, Academic Press, Inc, London, 1981.